**2020 IEEE International Symposium on
Safety, Security, and Rescue Robotics (SSRR)
November 4-6, Abu Dhabi, UAE**

Design and Map-based Teleoperation of a Robot for Disinfection of COVID-19 in Complex Indoor Environments

Dean Conte[1,3], Spencer Leamy[2,3] and Tomonari Furukawa[3]

***Abstract*— This paper presents the design and map-based teleoperation of a robot with ultraviolet-C (UVC) lamps that disinfects the COVID-19 virus in complex indoor environments. To disinfect a wide range of surfaces, the robot has an arm with six degrees-of-freedom in addition to a wheeled platform. The wheeled platform attaches tube lamps on each side and underneath in the orientation perpendicular to the moving direction, and the robot arm has a spot UVC lamp at its end-effector. A method for projecting surface dosage using light properties is proposed and validated using the sensor measurements from the robotic system. A technique for creating a disinfection map is presented to prove surface disinfection of the environment in three-dimensional space. The developed robot was tested in an indoor environment with typical structures. Experimental results demonstrate accurate disinfection map creation.**

I. Introduction

COVID-19 disease is a severe illness in humans observing exponential growth in almost all affected countries [1]. It is indispensable that COVID-19 be completely disinfected from indoor environments such as hospital patient and waiting rooms since many infections have occurred in such settings. Currently, COVID-19 is predominantly disinfected by humans using chemicals in complex indoor environments. Such laborious procedures cannot guarantee consistency and pose a great risk to human health. It is desirable to implement an unmanned solution that could improve the disinfection quality and decrease exposure risk [2].

Despite its significance, past work on robotic virus disinfection has been significantly limited. This is due to previous success with controlling past epidemics and pandemics such as SARS in 2003, Ebola outbreak in 2014 and MERS in 2015, which did not warrant the need to exploit robotic solutions. The most common type of virus disinfection robot has evolved from a commercially available ultraviolet-C (UVC)-based static machine. The static machine consists of circularly aligned vertical tube UVC lamps and disinfects the entire room including air [3]. The machines use high power lamps to ensure surface disinfection of the entire room over time.

The existing disinfection robots fully inherit the design and thus sees their novelty in the incorporation of a wheeled base and their autonomous navigation capability [4]–[6]. However, similar to the static machine, the robots can only quickly disinfect vertical surfaces of the room on line-of-sight (LOS). If there are objects and structures in the room, there will be many surfaces that cannot be disinfected thoroughly. However, the motion of the base does improve the disinfection capability.

Issues with robotic virus disinfection also exist with their operation. Some robots are designed for local teleoperation and limits the location of the operator [5]. Other robots can be remotely operated in a room to develop a two-dimensional (2-D) map and a defined path. Then, the autonomous capability simply follows the predefined path [7]. For disinfecting complex indoor environments, a 2-D map is insufficient at identifying and ensuring all the three-dimensional (3-D) surfaces are disinfected.

This paper presents the design and map-based teleoperation of a robot that disinfects the COVID-19 virus in complex indoor environments including hospital patient and waiting rooms. The robot consists of an unmanned ground vehicle (UGV) equipped with a six degrees-of-freedom (DOFs) manipulator. To disinfect various surfaces, the UGV has tube UVC lamps attached on each side and underneath orientated perpendicular to the moving direction. Additionally, the robot arm has a spot UVC lamp as its end-effector. The teleoperation proposed in this paper allows a human to operate the robot beyond the line-of-sight (LOS) simply by specifying robot waypoints on a dynamically constructed map. The two-stage mapping technique enables robot operation in an unknown environment and creates a fine disinfection map to ensure disinfection of all 3-D surfaces.

The paper is organized as follows. The next section describes virus disinfection by UVC light. The proposed robot design and fine disinfection map creation is presented in Section III. Section IV investigates the performance and capability of the developed robot, and conclusions and future work are summarized in Section V.

II. Virus Disinfection by UVC Energy

A. Coronavirus Characteristics

Many studies have shown that environmental contamination leads to infections. Some pathogens can survive for days to months whereas coronavirus, including SARS-CoV-2 or COVID-19, have been found to survive up to 5 days on certain surfaces. One of the effective methods to destroy bacteria, mold, viruses and other biological contaminants is UVC light with a wavelength of 253.7 nm. UVC light exposure kills biological contaminants in the air, liquids, or on surfaces by disrupting the outer membrane of microbes.

[1]Department of Mechanical Engineering, Virginia Tech, Blacksburg, VA, 24060 USA dconte97@vt.edu
[2]Corvus Labs, LLC Blacksburg, VA, 24060 USA spencer.leamy@corvuslabs.io
[3]Department of Mechanical and Aerospace Engineering, University of Virginia, Charlottesville, VA, 22904 USA tomonari@virginia.edu

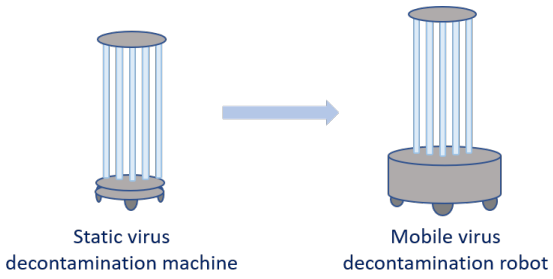

Fig. 1. Existing virus disinfection robots

Similar to the sound wave, the UVC energy is known to follow the inverse square law when evaluating its impact on a surface. The UVC energy on the surface, E, is given by

$$E = \frac{I}{L^2} \tag{1}$$

where I is the luminous intensity and L is the distance from the source to the surface. The model indicates that it is important that the UVC source be maintained close to the surface during disinfection.

B. Virus disinfection Robot with UVC Energy

Figure 1 shows a typical UVC-based robotic disinfection system and its evolution from a static machine. The aim is to disinfect the entire room including air by sufficiently projecting UVC light. The static machine consists of vertical tube UVC lamps aligned circularly. The design only permits static disinfection, so the machine is equipped with wheels for manual relocation. The disinfection robot fully inherits the static design and sees its novelty in the incorporation of a UGV and its autonomous navigation capability [4]. However, similar to the static machine, the robot can disinfect vertical surfaces of the room on LOS only. If there are objects and structures in the room, there will be many surfaces that are not on the LOS. Such surfaces can be disinfected only by reflection and will not be disinfected if reflectivity is low. In general, static disinfection with circularly aligned vertical lamps is energy inefficient and slow since high power and additional time is necessary when the environment contains surfaces that need to be disinfected through reflection.

C. Autonomous Virus disinfection by Mobile Robot

Figure 2 shows the schematic diagram of the existing robotic virus disinfection procedure. The primary aim is unmanned virus disinfection, so the first preprocess is the manual maneuvering of the robot for mapping of the environment on LOS. This is denoted as *remote control* and results in collecting sensor measurements including LiDAR/camera images. The next preprocess is 2-D mapping from the sensor measurements which yields a 2-D map of the environment. A 2-D path is then planned offline using the 2-D map. Note that 2-D mapping is sufficient as the path of the indoor environment is most conveniently determined in 2-D space. Once the path has been determined, the robot will perform autonomous virus disinfection by following the path.

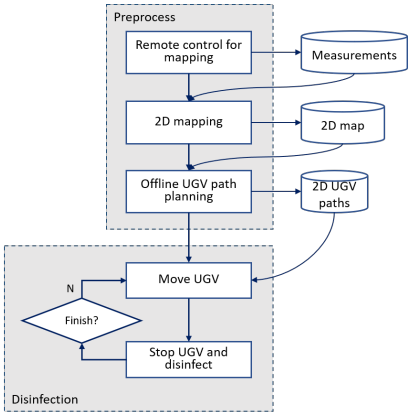

Fig. 2. Existing robotic virus disinfection procedure

While the framework is explained with "autonomous" capability, the system is not truly autonomous since the robot simply follows a path. Moreover, the determination of disinfection locations is subjective with no quantitative evaluation.

III. Virus Disinfection Robot

A. Robot Design and Teleoperation

The first innovation of the proposed approach lies in the design of the virus disinfection robot. Figure 3 shows the schematic diagram of the proposed design and the actual developed robot. The robot consists of two robotic modules: a UGV and an arm. The custom-built UGV is a rectangular solid shape as indoor environments are dominantly defined by orthogonal planes [8]. It attaches two vertical UVC tube lamps on each side and two horizontal tube UVC lamps underneath in the orientation perpendicular to the moving direction. These lamps sweep vertical surfaces and the floor while the robot moves. The robot uses four wheel drive four wheel steering to maximize maneuverability while minimizing unnecessary changes in orientation while operating. To disinfect other surfaces, the UGV has a robotic arm with six DOFs (Universal Robots UR10e). The spot UVC lamp attached to the end of the robot arm disinfects non-vertical and hidden surfaces. The robot is equipped with two cameras. A stereo camera is attached to the end of the arm to view and reconstruct the surrounding environment from various viewpoints and to share the same orientation with the spot UVC lamp. The fisheye lens camera is, on the other hand, used to monitor and teleoperate the robot and is fixed to the rear side of the robot.

Figure 4 shows the electronic diagram of the robot as well as the implementation of teleoperation. The UGV and the UR10e arm are controlled by the onboard computer. For virus disinfection, the tube lamps and the spot lamp are connected and also controlled by the onboard computer. Sensors of the robot include wheel encoders, robot joint encoders and an inertial measurement unit (IMU) in addition to the aforementioned cameras. The other unique feature of the proposed robot is the use of Long-Term Evolution

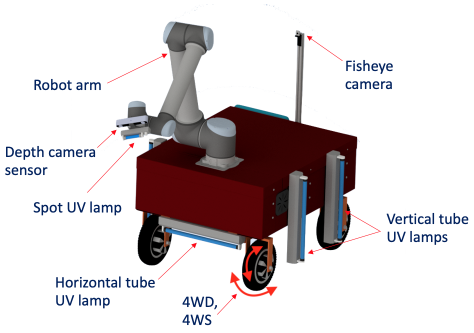

(a) Design

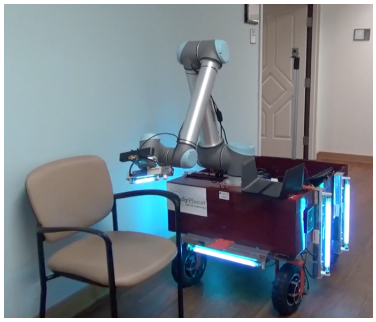

(b) Development

Fig. 3. Proposed virus disinfection robot

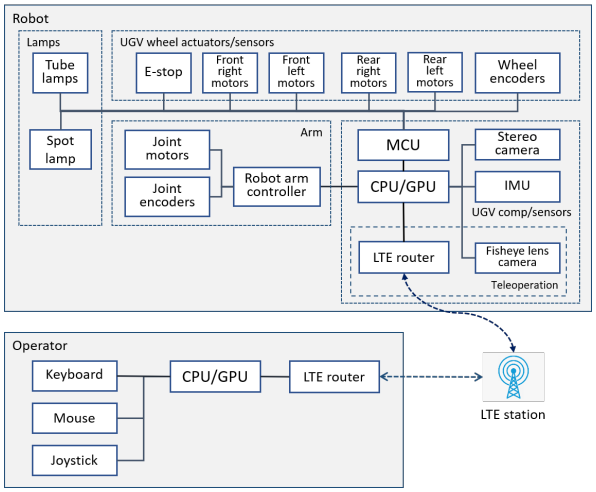

Fig. 4. Electronic diagram and teleoperation

(LTE) signals for wireless communication. Using LTE allows for reliable and stable teleoperation independent of local networks. This is critical as hospital Wi-Fi networks connect various sensitive medical equipment and a poor connection affects the safety, speed and range of the proposed system.

B. Disinfection Procedure Incorporating Two-Stage Mapping

Figure 5 shows the procedure of the proposed robotic virus disinfection with two-stage mapping. Due to the reliable and stable teleoperation, the robot develops a map of the environment beyond the LOS. Since the surfaces in need of

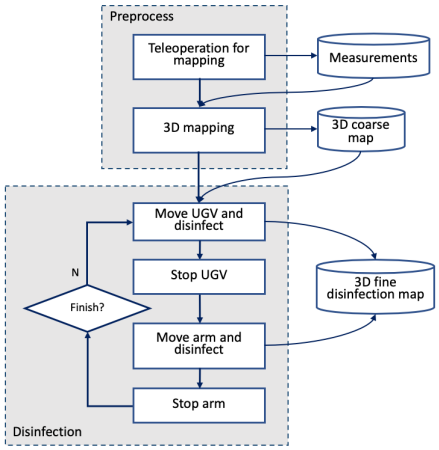

Fig. 5. Proposed procedure

disinfecting are three-dimensionally oriented, a 3-D map is first created by driving the robot in the environment keeping distance from the walls and other object surfaces. This "coarse" map is then used to identify surfaces to disinfect. Coarse 3-D mapping has been extensively studied over the last two decades, and can be conducted using a Simultaneous Localization and Mapping (SLAM) technique with loop closure or a Structure-from-Motion (SfM) technique with Bundle Adjustment (BA) [9], [10].

The fine mapping and disinfection process begins by teleoperating the UGV in the environment this time at a closer distance the surfaces so effective disinfection can occur. The floor and vertical surfaces are disinfected when the UGV moves and the map showing the disinfected surfaces in finer resolution is updated at every timestep. To efficiently show the surface, a surface map is generated by representing the cloud of points with voxels. When the robot comes across non-vertical surfaces, the UGV is stopped and the arm then moves to disinfect the surfaces. The "fine" disinfection map is updated again during the disinfection process. The robot returns to navigating via teleoperation once the disinfection of the non-vertical surfaces has been completed.

The strength of the proposed teleoperation lies in the use of the disinfection map. Since the disinfected surfaces are identified, the proposed virus disinfection does not leave surfaces until they are fully disinfected. Additionally, the proposed approach stores the coarse map for reuse allowing for slight changes in the environment between disinfections which is important for environments such as hospital rooms and offices.

C. Disinfection Map

The purpose of the disinfection map is to determine if there is enough UVC dosage projected onto the surface of concern to kill the virus. Figure 6 illustrates the UVC dosage given to a point of surface positioned when the UVC light is crossing over the surface. Let the light source be oriented with the point at position $\mathbf{x}_k$ by angle θ_k at time step k. The luminous intensity with the angle, $I(\theta)$, is non-zero if

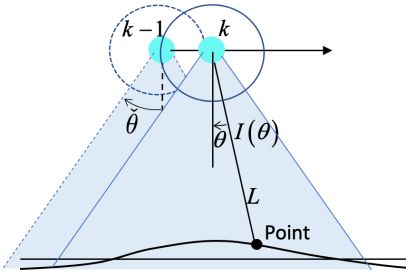

Fig. 6. UVC dosage given to a point of surface

the angle is within the range of light distribution. Given the light projected onto the surface with distance L_k, the UVC energy E_k is given by

$$E_k = \begin{cases} \frac{I(\theta_k)}{L_k^2} & |\theta_k| \leq \breve{\theta} \\ 0 & \text{Otherwise} \end{cases} \quad (2)$$

where $\breve{\theta}$ is the maximum angle defining the light distribution range. Since the UVC lamps used are cylindrical shaped and therefore omnidirectional, the luminous intensity is constant for each angle within $\breve{\theta}$. Therefore, $\breve{\theta}$ is defined by the geometry of mounting position.

The point receives the UVC energy continuously while the light source keeps moving. The cumulative UVC energy that the point receives up to time step k, or the UVC dosage, is incrementally derived as

$$\Phi_k(\mathbf{x}) = \Phi_{k-1}(\mathbf{x}) + E_k \Delta t \quad (3)$$

For computational efficiency, the surface is evaluated by discrete elements. The average UVC dosage of element e is given by

$$\Phi_k^e = \frac{1}{A_k^e} \int_{\mathcal{X}^e} \Phi_k(\mathbf{x}^e) \mathrm{d}\mathbf{x}^e \quad (4)$$

The targeted teleopration provides the UVC light until the average UVC dosage exceeds the threshold, which secures the disinfection of virus:

$$\Phi_k^e \geq \breve{\Phi}^e \quad (5)$$

The threshold for 99.9% sterilization of SARS virus family using direct UVC light with a wavelength of 254nm is known to be 10-20mJ/cm^2 [11].

Algorithm 1 shows the methodology used to add voxels to the disinfection map. The function ComputeDosage() computes the estimated dosage at each each voxel based on UVC light intensity and the distance from the lamps. The function DisinfectionVoxel(V) outputs all the voxels that lie within the area of effect of the UV light disinfection. At each timestep, voxels that lie within the area of effect of the UV light disinfection are identified. Then dosage at each voxel is estimated based on the mathematics presented in this section. Finally, each voxel is compared to the UVC dosage threshold to determine if it should be added to the disinfection map.

Algorithm 1: Disinfection Map Update Algorithm

```
Result: voxel disinfection map
function ComputeDosage();
function DisinfectionVoxel(V);
initialize DisinfectionMap(VD) := (t - 1);
while True do
    t := current time;
    for each voxel V(x_i, y_i, z_i) in grid do
        if DisinfectionVoxel(V(x_i, y_i, z_i)) then
            V(x_i, y_i, z_i) :=
              ComputeDosage(V(x_i, y_i, z_i));
            if ComputeDosage(V(x_i, y_i, z_i)) < Φ̆^e
              then
                return V(x_i, y_i, z_i)
            else
                if ComputeDosage(V(x_i, y_i, z_i)) ≥ Φ̆^e
                  then
                    store voxel(V(x_i, y_i, z_i)) →
                      DisinfectionMap(VD)
                end
            end
        end
    end
end
```

IV. Numerical/Experimental Validation

The efficacy of the proposed virus disinfection was investigated in three steps. The first step investigates the accuracy of the UVC dosage Eqs. (2)-(4) by comparing the theoretical dosage to ground truth dosage measured with a handled UVC sensor placed at various distances. The second step examines the performance of disinfecting typical structures by the movement of the UGV and the arm. In the final step, the capability of developing the 3-D disinfection map was validated. The UVC lamps were kept on to construct a disinfection map in a real scene.

A. UVC Projection Evaluation

The validity of Eq. 2 was first evaluated since all subsequent Eqs. and Algorithms depend on its correctness. Only one UVC lamp on the UGV or the arm was kept on at a time for the Eq. 2 validation. Figure 7 shows the dosage measured at varying distances for the large vertical lamps and the small spot lamp. The UVC dosage measured by the handheld sensor is shown to greatly overestimate the theoretical curve. This result is reasonable since Eq. 2 assumes the light is an omnidirectional point source, not an omnidirectional linear source. The reflective lamp ballast and UGV side paneling also provides additional dosage. Therefore, a curve fit of experimental data found more precise dosage equations for

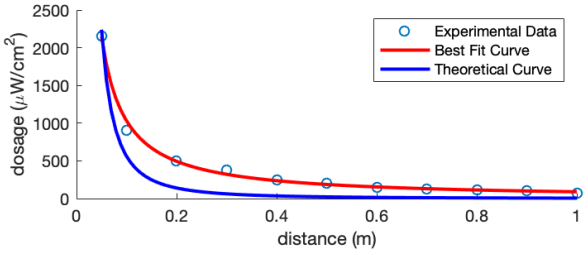

(a) Vertical Lamp

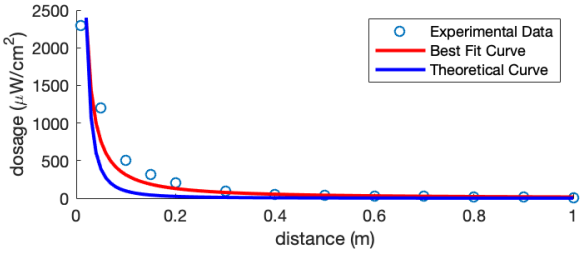

(b) Spot Lamp

Fig. 7. Evaluation of UVC projection

(a) Filing cabinet (b) Chair

Fig. 8. Structures for evaluating disinfection performance

our specific application to be:

$$E_k^{vertical} = \frac{I^{vertical}(\theta_k)}{L_k^{1.06}} \tag{6a}$$

$$E_k^{spot} = \frac{I^{spot}(\theta_k)}{L_k^{1.27}} \tag{6b}$$

when $|\theta_k| \leq \check{\theta}$. $I^{vertical}(\theta_k)$ and $I^{spot}(\theta_k)$ were experimentally found to be 89.75 and 16.73 μW/cm^2 respectively. Eq. 6 replaces Eq. 2 in the subsequent sections.

B. Disinfection Performance of Structures

To validate the creation of the disinfection map described in Algorithm 1, two structures were disinfected and measured with a handheld device in parallel. Figure 8 shows two structures used to investigate the performance. The first structure is a filing cabinet with drawers placed against a wall. The filing cabinet is occasionally touched and will be disinfected by the UGV. The second structure is a chair, which will be disinfected by the arm as there are various non-vertical high-touch surfaces.

Table I lists the parameters used for the 3-D reconstruction.

TABLE I
PARAMETERS

Parameter	Coarse map	Fine map
UGV distance to cabinet	2 [m]	∼50 [cm]
Arm distance to chair	-	∼30 [cm]
Voxel resolution	50 [mm]	10 [mm]

A coarse map was created *a priori* with the UGV kept to 2m from the filing cabinet and chair. In the fine mapping and disinfection, the robot was navigated closely to the structures since the aim of navigation is disinfection. The distance of the UGV to the filing cabinet was dynamic but roughly constant at 50cm. The distance of the arm end effector to the chair was also dynamic but kept to approximately 30cm.

Figure 9 shows the dosage estimated by Algorithm 1 and the measured dosage over time at a specific voxel indicated by red stars in Fig. 8. Disinfection of the cabinet in Fig. 9(a) evaluates a single vertical lamp with dynamic motion, and confirms the proposed algorithm is effective in estimating true dosage to surfaces which are parallel to the orientation of the UGV. Similarly, Fig. 9(b) evaluates dosage received by a chair arm. However, the measured dosage from the static sensor is significantly below the estimated dosage from the proposed approach. Possible causes include the affect of the orientation of the UVC sensor. I.e. if the sensor is held perpendicular to the light source, the dosage matches the algorithm much closer. This result indicates that the surface orientation should be taken into account to improve the estimation accuracy.

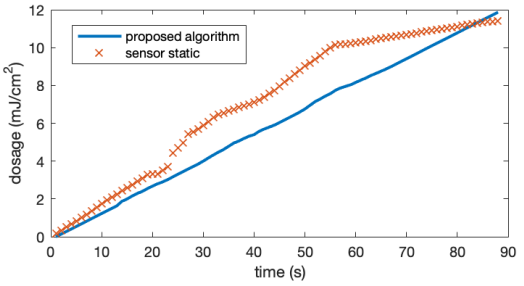

(a) Cabinet

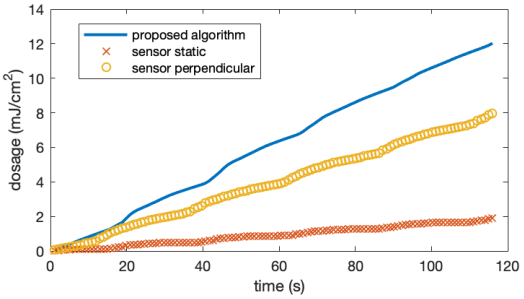

(b) Chair

Fig. 9. Evaluation of UVC disinfection algorithm using objects

To verify the influence of the orientation, Figure 10 shows the measured dosage at a fixed distance of 60cm, but varying

angle θ_k. The data was collected with the sensor oriented facing the light source (the assumption made in this paper), and with the sensor perpendicular to the UGV. The results indeed indicate the dosage relies on the incidence angle of the surface.

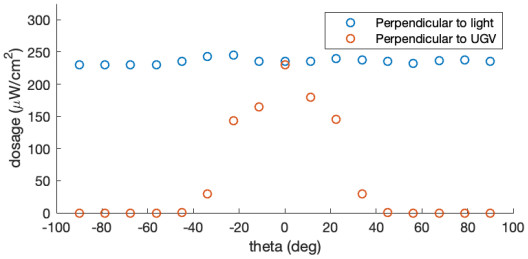

Fig. 10. Evaluation of light incidence angle

C. 3-D Disinfection Map of the Entire Space

To develop the 3-D disinfection map, the arm and UGV were first moved to generate the coarse map. Then the UGV is moved, a fine map is generated, and Algorithm 1 is run with a Δt of 1s. Figure 11 shows a series of screenshots demonstrating the proposed technique. The blue color indicates the surface dosage of the voxel is above the threshold. The disinfection map of Figure 11 is shown with some colored points for visualization purposes. The noted advantage of the proposed technique is the ability to create a proven disinfection map. Unlike the human cleaner who disinfects surfaces through their memory, the proposed technique can disinfect surfaces reliably by registering all the disinfected surfaces.

V. Conclusions

This paper has presented the design of a robot with UVC lamps that disinfects the COVID-19 virus in complex indoor environments while creating a disinfection map. To disinfect a wide range of surfaces, the robot has an arm in addition to a wheeled platform. In addition to allowing a human to operate the robot beyond the LOS, the proposed technique implements two-stage mapping approach to develop a coarse map for teleoperation and a high-resolution disinfection map to ensure decontamination on all surfaces. The developed robot was tested in an indoor environment and the results show the proposed method is effective in creating a fine disinfection map.

This paper reports the first progress of the authors on robotic virus disinfection. The robot and proposed method needs various advancements. Most importantly, the work presented here illustrates the importance of including light incidence angle on surfaces for true surface dosage estimation. Ongoing work also includes the use of an UVC camera to measure the UVC dosage and the operation of the robot with an improved level of autonomy.

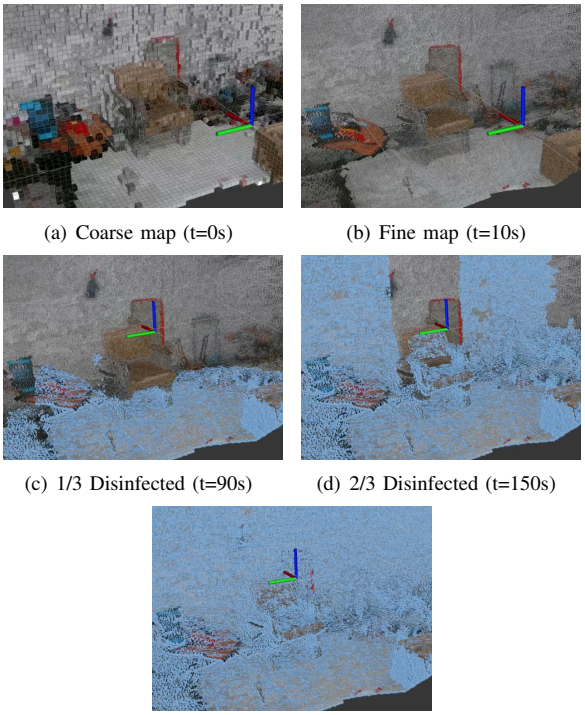

(a) Coarse map (t=0s) (b) Fine map (t=10s)

(c) 1/3 Disinfected (t=90s) (d) 2/3 Disinfected (t=150s)

(e) Disinfection map (t=270s)

Fig. 11. 3-D disinfection procedure

Acknowledgement

This work is sponsored by US Office of Naval Research (N00014-20-1-2468). The authors would like to express their sincere gratitude to Dr. Tom McKenna for his invaluable support and advice.

References

[1] "Severe outcomes among patients with coronavirus disease 2019 (covid-19) — united states, februry 12–march 16, 2020," MMWR Morb Mortal Wkly Rep 2020, vol. 69, no. 343-346, 2020.

[2] G.-Z. Yang, B. J. Nelson, R. R. Murphy, H. Choset, H. Christensen, S. H. Collins, P. Dario, K. Goldberg, K. Ikuta, N. Jacobstein, D. Kragic, R. H. Taylor, and M. McNutt, "Combating covid-19—the role of robotics in managing public health and infectious diseases," Science Robotics, vol. 5, no. 40, 2020.

[3] N. Mahida, N. Vaughan, and T. Boswell, "First uk evaluation of an automated ultraviolet-c room decontamination device (tru-d™)," Journal of Hospital Infection, vol. 84, no. 4, pp. 332 – 335, 2013.

[4] P. Chanprakon, T. Sae-Oung, T. Treebupachatsakul, P. Hannanta-Anan, and W. Piyawattanametha, "An ultra-violet sterilization robot for disinfection," in 2019 5th International Conference on Engineering, Applied Sciences and Technology (ICEAST), pp. 1–4, 2019.

[5] M. Bentancor and S. Vidal, "Programmable and low-cost ultraviolet room disinfection device," HardwareX, vol. 4, p. e00046, 2018.

[6] M. Guettari, I. Gharbi, and S. Hamza, "Uvc disinfection robot," Environmental Science and Pollution Research, 2020.

[7] E. Ackerman, "Autonomous robots are helping kill coronavirus in hospitals," IEEE Spectrum, 2020.

[8] O. Saurer, F. Fraundorfer, and M. Pollefeys, "Homography based visual odometry with known vertical direction and weak manhattan world assumption," 2012.

[9] M. Labbé and F. Michaud, "Rtab-map as an open-source lidar and visual simultaneous localization and mapping library for large-scale and long-term online operation," Journal of Field Robotics, vol. 36, no. 2, pp. 416–446, 2019.

[10] R. Shah, A. Deshpande, and P. J. Narayanan, "Multistage sfm: A coarse-to-fine approach for 3d reconstruction," 2016.

[11] A. Bianco, M. Biasin, G. Pareschi, A. Cavalleri, C. Cavatorta, C. Fenizia, P. Galli, L. Lessio, M. Lualdi, E. Redaelli, I. Saulle, D. Trabattoni, A. Zanutta, and M. Clerici, "Uv-c irradiation is highly effective in inactivating and inhibiting sars-cov-2 replication," medRxiv, 2020.